Expanded View Figures

Figure EV1. Characteristics of 100K-EVs isolated from THP-1 cells.

A Extracellular mtDNA leakage from human peripheral blood leukocytes following LPS stimulation. White blood cells isolated from peripheral blood by removing red blood cells were stimulated with LPS (500 ng/ml) for 4 h. DNA was purified from the CS, and the levels of mtDNA were measured using qPCR.

B Transmission electron microscopic image of 100K-EVs. 100K-EVs isolated from the CS of pyroptotic THP-1 cells were attached to the coverslip and visualized using transmission electron microscopy. Scale bar, 200 nm.

C Particle sizes of 16K-EVs (upper) and 100K-EVs (lower) isolated from CS of WT THP1 cells.

D Expression of representative exosome markers in 100K-EVs. 100K-EVs isolated from the CS of pyroptotic THP-1 cells were lysed, and the levels of CD9, CD63, and Flotillin were evaluated using western blotting.

E Amount of 100K-EVs used in each experiment. 100K-EVs isolated from CS of confluent WT THP1 cells in 10 cm culture dishes were quantified by CD63-specific ELISA.

F, G Generation of mtDNA-defective THP-1 (ρ0 THP-1) cells. ρ0 THP-1 cells were established by culturing WT THP-1 cells with medium containing a low concentration of Ethidium Bromide. The absence of mtDNA in ρ0 THP-1 cells (F) and 100K-EVs released upon LPS plus ATP stimulation (G) was confirmed using qPCR.

H, I Equivalent secretion of 100K-EVs and TNF-α in ρ0 THP1 cells. The amount of 100K-EVs and TNF-α in CS of WT and ρ0 THP1 cells stimulated with ATP or LPS were measured by western blotting (H) and the reporter cells for TNF-α (I).

J The level of dsDNA in 100K-EVs. dsDNA was purified from 100K-EVs of WT and ρ0 THP1 cells, and the amount of dsDNA was quantified using the Quant-iT dsDNA Assay Kit.

Data information: Statistical analyses were performed using a Mann–Whitney *U* test (A: median; 25^{th} and 75^{th} percentile; minimum and maximum value excluding population outliers; $^{**}P < 0.01$), a Student's *t*-test (F: mean ± SD; $^{**}P < 0.01$), a Mann–Whitney *U* test (J: mean ± SD; $^{*}P < 0.05$), or an ANOVA with Tukey's *post-hoc* test (G–I) (mean ± SD; $^{*}P < 0.05$, $^{**}P < 0.01$; NS, not statistically significant). For panel E, (mean ± SD). The data are representative of two (B, C) three (A, D–J) independent experiments.
Source data are available online for this figure.

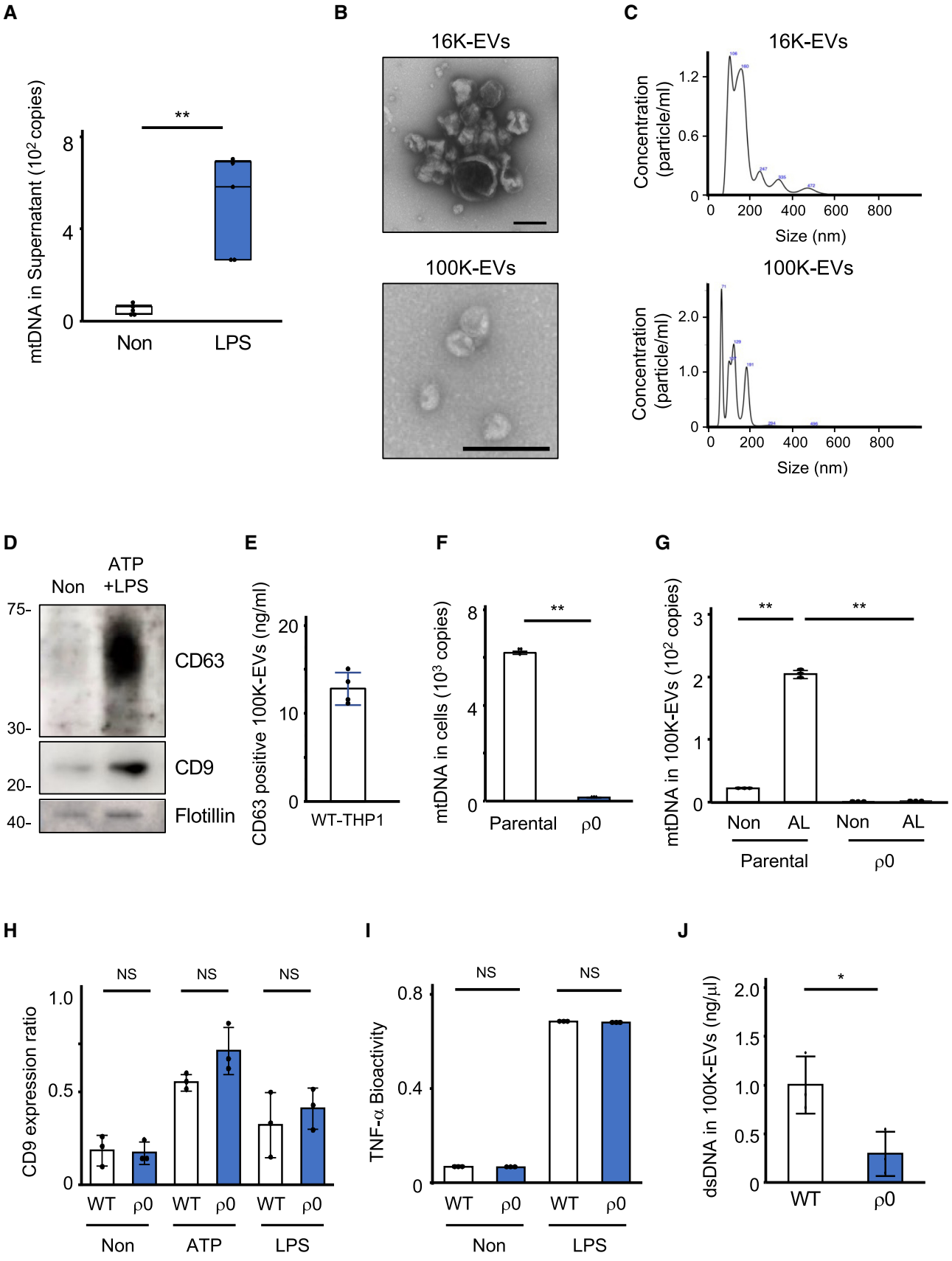
A
mtDNA in Supernatant (10² copies)
**
Non
LPS
B
16K-EVs
100K-EVs
C
16K-EVs
Concentration (particle/ml)
Size (nm)
100K-EVs
Concentration (particle/ml)
Size (nm)
D
Non
ATP +LPS
75-
30-
20-
40-
CD63
CD9
Flotillin
E
CD63 positive 100K-EVs (ng/ml)
WT-THP1
F
mtDNA in cells (10³ copies)
**
Parental
ρ0
G
mtDNA in 100K-EVs (10² copies)
**
**
Non
AL
Non
AL
Parental
ρ0
H
CD9 expression ratio
NS
NS
NS
WT
ρ0
WT
ρ0
WT
ρ0
Non
ATP
LPS
I
TNF-α Bioactivity
NS
NS
WT
ρ0
WT
ρ0
Non
LPS
J
dsDNA in 100K-EVs (ng/μl)
*
WT
ρ0

Figure EV1.

Figure EV2. Establishment of mtDNA-defective, caspase-1-deficient, or gasdermin-D-deficient THP-1 cells.

A Localization of mtDNA and mitochondria. Parental and ρ0 THP-1 cells were stained with the PicoGreen (green) and MitoTracker-Deep Red (red) dyes and visualized using confocal microscopy. Scale bar, 10 μm.

B, C Establishment of Casp1-KO and Gsdmd-KO-THP-1 cells. Caspase-1 levels in parental WT and Casp1-KO-THP-1 cells (B) and gasdermin-D in parental WT and Gsdmd-KO-THP-1 cells (C) were evaluated using western blotting using anti-caspase-1 (B) and anti-gasdermin-D (C) antibodies.

D, E Equivalent mitochondrial homeostasis in steady-state Casp1-KO and Gsdmd-KO-THP-1 cells. Cellular mtDNA levels (D) and distribution of mtDNA and mitochondria (E) in parental WT, Casp1-KO, and Gsdmd-KO-THP-1 cells at the steady-state. Scale bar, 5 μm.

F, G IL-1β and LDH release by Casp1-KO and Gsdmd-KO-THP-1 cells. Release of IL-1β (F) and LDH (G) from parental WT, Casp1-KO, and Gsdmd-KO-THP-1 cells upon pyroptosis-inducing stimulation.

H Separation of cytoplasmic and mitochondrial fractions. After the removal of nuclei from WT, Caps1-KO, and Gsdmd-KO THP1 cells stimulated with LPS and ATP, the mitochondrial fraction was separated. The remaining fraction was designated the cytosol fraction. The expression of the proteins shown in the figure in each fraction was evaluated by western blotting.

I–K Restoration of full-length caspase-1 in Casp1-KO-THP-1 cells. FLAG-tagged full-length caspase-1 was transduced via lentivirus into Casp1-KO (FL-Casp1-Casp1-KO) THP-1 cells. Pro-caspase-1 and FLAG expression levels in parental WT, Casp1-KO, and FL-Casp1-Casp1-KO-THP-1 cells were evaluated using western blotting (I). The levels of IL-1β (J) and LDH (K) in the supernatant were also evaluated.

L Evaluation of STING's involvement. The level of mtDNA in 100K-EVs (left) and IL-1β (right) in CS of WT and STING-KO THP1 upon LPS plus ATP simulation was determined.

Data information: Statistical analyses were performed using an ANOVA with Tukey's *post-hoc* test (D, F, G, J–L) (mean ± SD; $*P < 0.05$, $**P < 0.01$; NS, not statistically significant). The data are representative of two (A–H, I–K) and three (L) independent experiments.
Source data are available online for this figure.

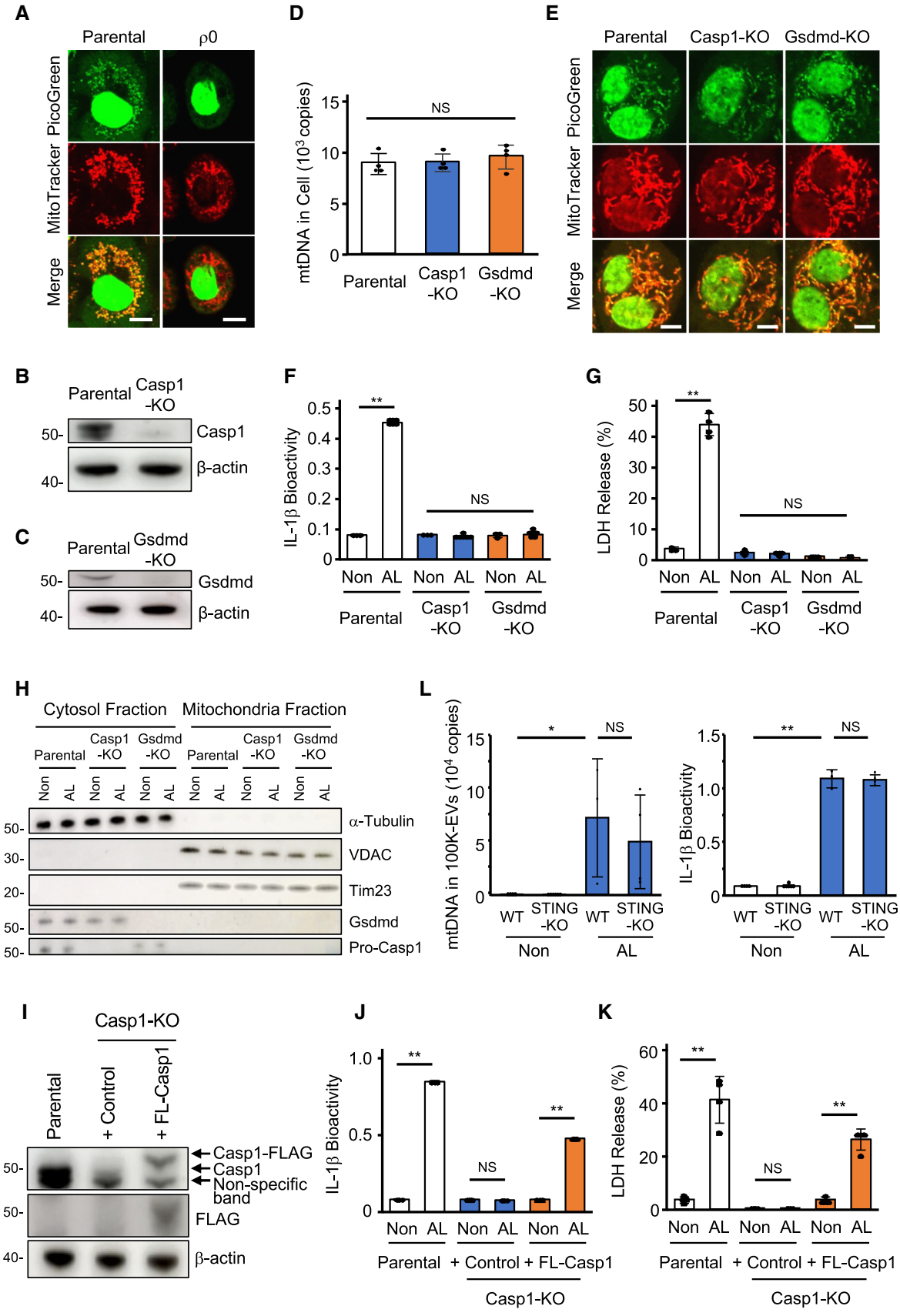
A
Parental
ρ0
PicoGreen
MitoTracker
Merge
D
mtDNA in Cell (10^3 copies)
NS
Parental
Casp1 -KO
Gsdmd -KO
E
Parental
Casp1-KO
Gsdmd-KO
PicoGreen
MitoTracker
Merge
B
Parental
Casp1 -KO
50-
Casp1
40-
β-actin
C
Parental
Gsdmd -KO
50-
Gsdmd
40-
β-actin
F
IL-1β Bioactivity
**
NS
Non AL Non AL Non AL
Parental
Casp1 -KO
Gsdmd -KO
G
LDH Release (%)
**
NS
Non AL Non AL Non AL
Parental
Casp1 -KO
Gsdmd -KO
H
Cytosol Fraction
Mitochondria Fraction
Parental
Casp1 -KO
Gsdmd -KO
Non AL
50-
α-Tubulin
30-
VDAC
20-
Tim23
50-
Gsdmd
50-
Pro-Casp1
L
mtDNA in 100K-EVs (10^4 copies)
*
NS
WT STING -KO WT STING -KO
Non
AL
IL-1β Bioactivity
**
NS
WT STING -KO WT STING -KO
Non
AL
I
Casp1-KO
Parental
+ Control
+ FL-Casp1
50-
Casp1-FLAG
Casp1
Non-specific band
50-
FLAG
40-
β-actin
J
IL-1β Bioactivity
**
NS
**
Non AL Non AL Non AL
Parental
+ Control
+ FL-Casp1
Casp1-KO
K
LDH Release (%)
**
NS
**
Non AL Non AL Non AL
Parental
+ Control
+ FL-Casp1
Casp1-KO

Figure EV2.

Figure EV3. Assessment of nuclear DNA and microvesicles' involvement in 100K-EV-induced inflammation.

A Establishment of NLRP3-KO-THP-1 cells. NLRP3-KO-THP-1 cells were generated using the CRISPR/Cas9 system. Expression of NLRP3 was assessed using western blotting with an anti-NLRP3 antibody (upper). IL-1β production by parental WT- and NLRP3-KO-THP-1 cells in response to LPS, ATP, MSU, and poly:dAdT (lower).

B Establishment of TLR9-expressing THP-1 cells. Human TLR9 was introduced into THP-1 cells by lentiviral transduction (TLR9-Ex). Expression of TLR9 was assessed using western blotting with an anti-TLR9 antibody (upper). TNF-α production induced by TLR9 ligands, such as K3 and ODN2006, was elevated in TLR9-Ex THP-1 cells (lower).

C Assessment of cGAS–STING involvement in 100K-EV-induced cytokine production. 100K-EVs isolated from CS of WT THP1 cells undergoing pyroptosis were added to WT or STING-KO THP1 cells. The level of IL-1β (left), IL-23 (middle), and IFN-I (right) was quantified using the specific reporter cells for these cytokines.

D Exosomes and microvesicles in 100K-EVs. 100K-EVs were isolated from CS of WT and Casp1-KO THP1 cells undergoing pyroptosis, the level of exosomes and microvesicles were evaluated by Western blotting (left) using anti-CD9 (middle) and anti-Na^+/K^+ ATPase (right) antibodies.

E, F Inflammation caused by 100K-EVs of Casp1-KO THP1 cells. 100K-EVs isolated from CS of WT and Casp1-KO THP1 cells undergoing pyroptosis were injected into the ankle of WT mice (E) and added to WT THP1 cells (F). The evaluation of ankle swelling (upper) and histological analysis (lower) was performed after 18 h. Scale bar, 1 mm. Quantitative data from the swollen ankle are shown on the right (E). IL-1β bioactivity in CS was measured using reporter cells for IL-1β (F).

Data information: Statistical analyses were performed using a Mann–Whitney *U* test (D), (median; minimum and maximum value excluding population outliers; $^{**}P < 0.01$; NS, not statistically significant), an ANOVA with Tukey's *post-hoc* test (C, F) (mean ± SD; $^{*}P < 0.05$, $^{**}P < 0.01$; NS, not statistically significant), or a Steel–Dwass test (E) (median; 25th and 75th percentile; minimum and maximum value excluding population outliers; $^{*}P < 0.05$; NS, not statistically significant). For panel A and B, mean ± SD. The data are representative of two (A, B, D–F) and three (C) independent experiments.
Source data are available online for this figure.

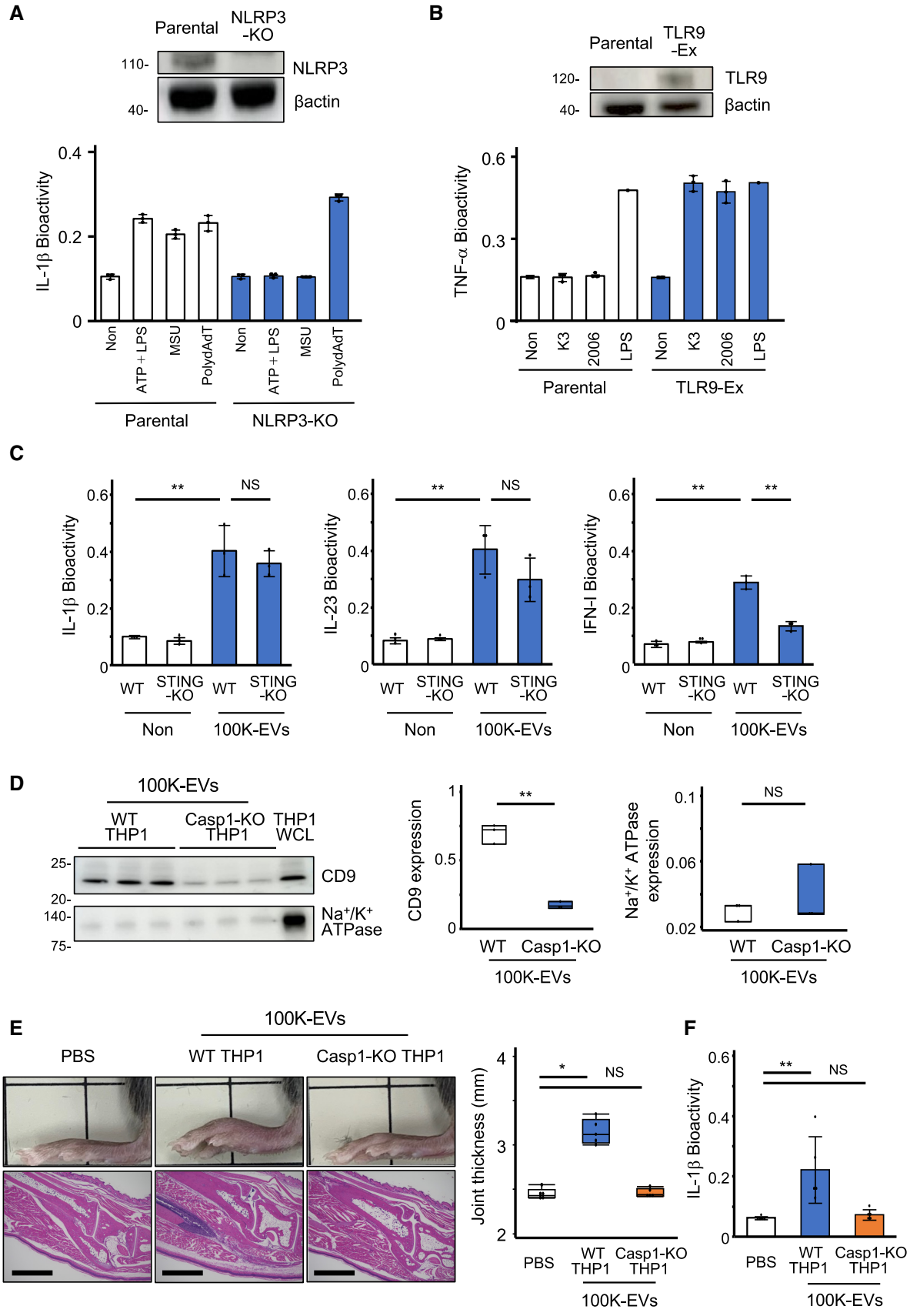

Figure EV3.

Figure EV4. Relationship between serum mtDNA levels and BS symptoms and characteristics of 100K-EVs purified from human sera.

A Serum IL-1β bioactivity. Serum IL-1β levels in BS, RA, and SjS were evaluated using the reporter cells for IL-1β.

B–G Relationship between serum mtDNA levels and BS symptoms. Serum mtDNA levels in BS patients were compared between asymptomatic patients and patients who exhibited any of the following symptoms on the sampling date: oral ulcers (B), uveitis (C), genital ulcers (D), skin lesions (E), arthralgia (F), and intestinal lesions (G).

H Degradation of mtDNA added to the serum by DNase I. mtDNA was spiked into the BS serum and digested by DNase I.

I–L Characterization of EVs isolated from serum. Particle sizes of 16K-EVs (I) and 100K-EVs (J) isolated from HC (upper) or BS serum (lower). Representative exosome markers, such as CD9, CD63, and Flotillin 1, but not calnexin, apolipoprotein-A1, or β-actin, were present in 100K-EVs isolated from serum (K). 100K-EVs isolated from BS serum were attached to a coverslip and visualized through transmission immunoelectron microscopy using an anti-CD9 primary antibody and a secondary antibody conjugated to 10-nm gold particles. Scale bar, 200 nm (upper) and 50 nm (lower) (L).

M Plasma mtDNA levels in 100K-EVs. 100K-EVs were isolated from HC and BS plasma, and DNA was purified. The mtDNA levels in 100K-EVs were measured using qPCR.

Data information: Statistical analyses were performed using a Mann–Whitney *U* test (B–G, M) (median; 25^{th} and 75^{th} percentiles; minimum and maximum value excluding outliers; $*P < 0.05$, $**P < 0.01$) or a Steel–Dwass test (A, H) (median; 25^{th} and 75^{th} percentile; minimum and maximum value excluding population outliers; $*P < 0.05$; NS, not statistically significant). The data are representative of two (M) and three (H) independent experiments.
Source data are available online for this figure.

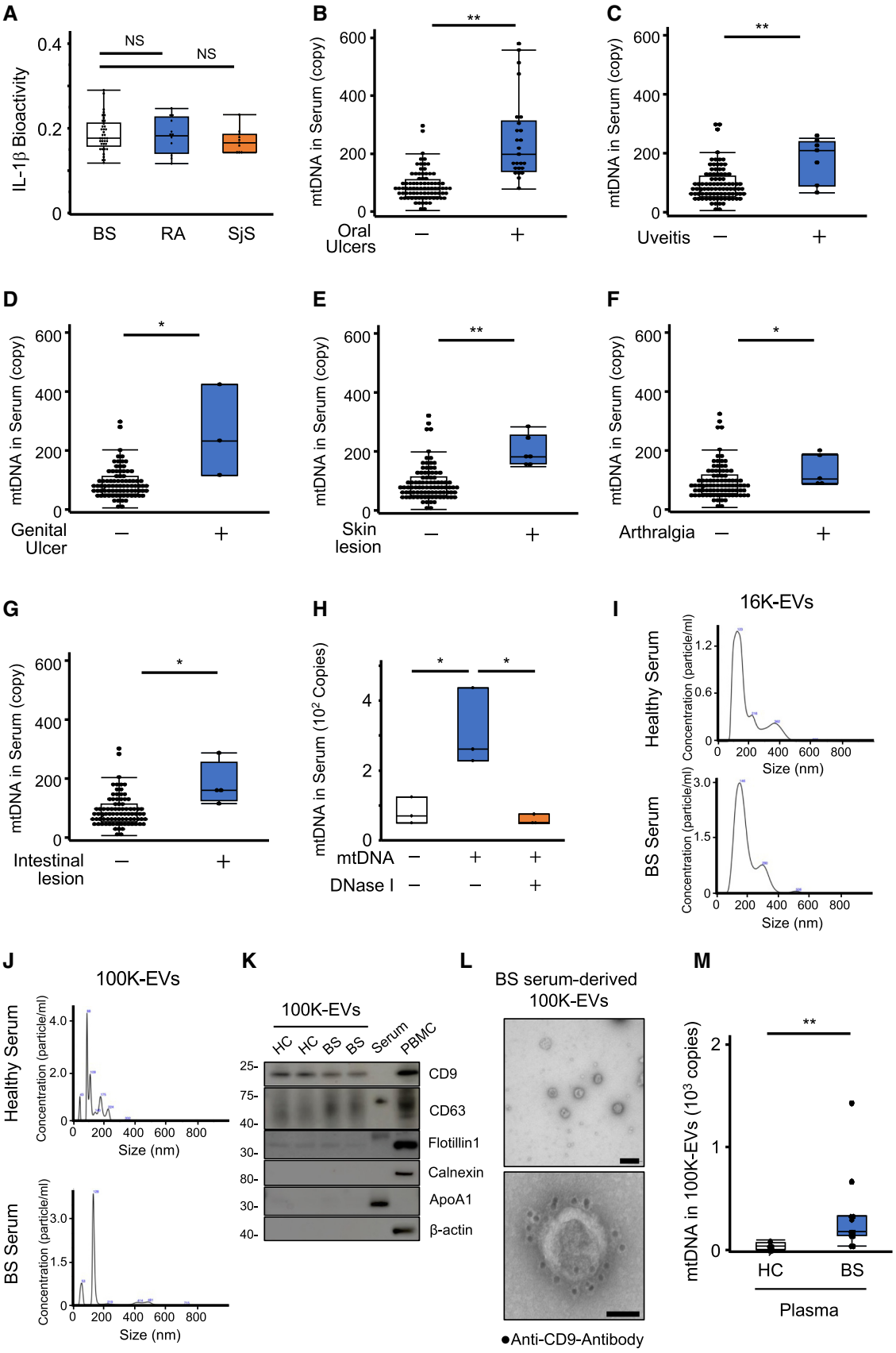

Figure EV4.

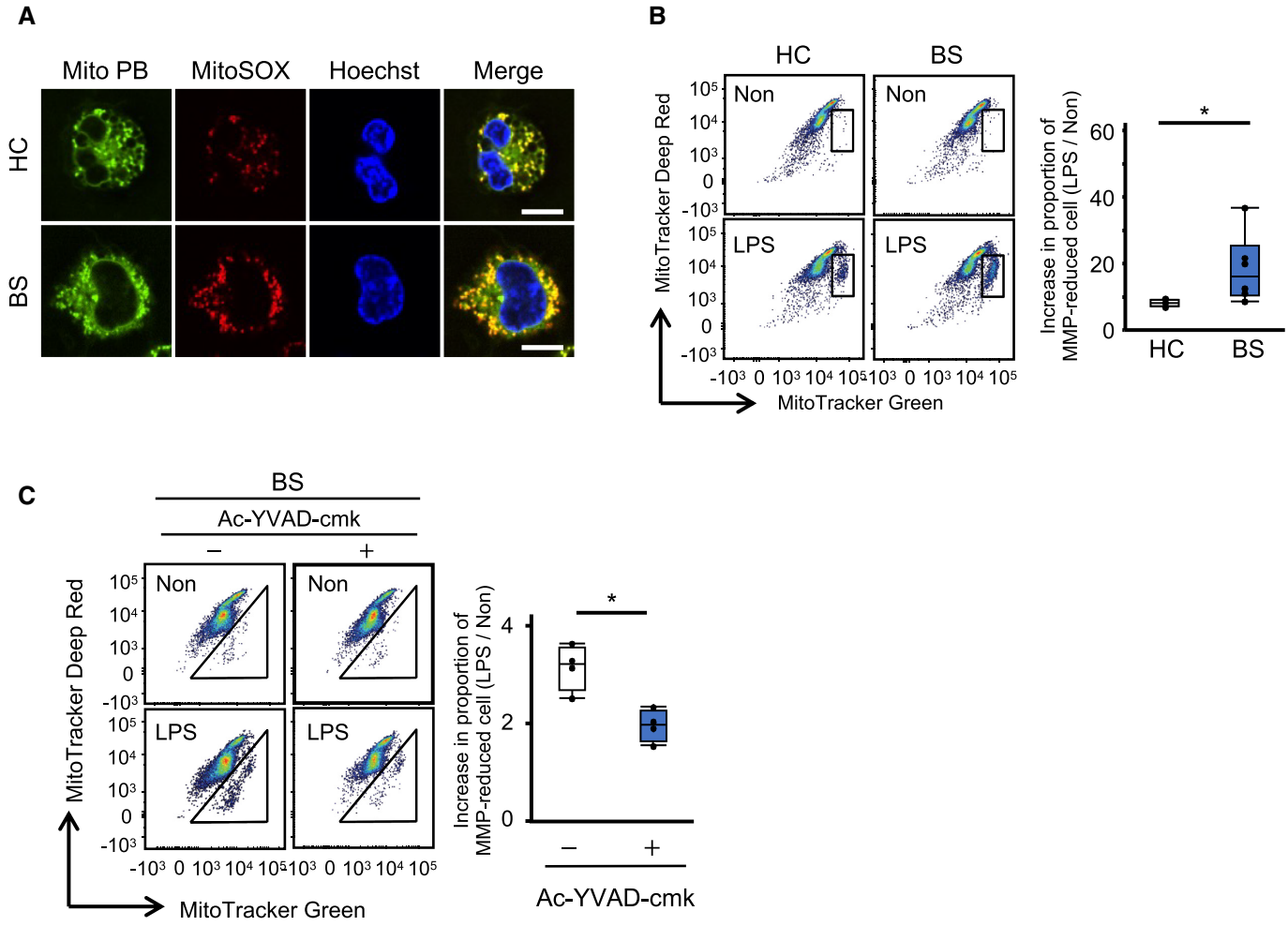

Figure EV5. Increased mitochondrial damage in BS monocytes.

A mROS production in CD14$^+$ monocytes. HC and BS monocytes were stained with MitoPB (green) and MitoSox (red), and mROS production was visualized using confocal microscopy. Scale bar, 5 μm.

B Mitochondrial membrane potential in CD14$^+$ monocytes. HC- and BS-derived CD14$^+$ monocytes were stimulated with LPS, and the reduction in the MMP was monitored by FACS using MitoTracker Green (X-axis) and MitoTracker-Deep Red (Y-axis) (left). The increase in the proportion of MMP-reduced cells (gated population) following LPS stimulation was quantified (right).

C Effect of caspase-1 on the increasing MMP of BS monocytes. BS-derived CD14$^+$ monocytes were stimulated with LPS in the presence or absence of Ac-YVAD-cmk, and the reduction in the MMP was monitored using FACS.

Data information: Statistical analyses were performed using a Mann–Whitney *U* test (B, C) (median; 25th and 75th percentiles; minimum and maximum value excluding outliers; *$P < 0.05$). The data are representative of two (A) and three (B, C) independent experiments.
Source data are available online for this figure.